

Dieu Tien Bui · Anh Ngoc Do  
Hoang-Bac Bui · Nhat-Duc Hoang  
*Editors*

# Advances and Applications in Geospatial Technology and Earth Resources

Proceedings of the International  
Conference on Geo-Spatial Technologies  
and Earth Resources 2017

 Springer

# Advances and Applications in Geospatial Technology and Earth Resources

Dieu Tien Bui · Anh Ngoc Do  
Hoang-Bac Bui · Nhat-Duc Hoang  
Editors

# Advances and Applications in Geospatial Technology and Earth Resources

Proceedings of the International Conference  
on Geo-Spatial Technologies and Earth  
Resources 2017



Springer

*Editors*

Dieu Tien Bui  
GIS group, Department of Business and IT  
University College of Southeast Norway  
Boskogen, Telemark  
Norway

Hoang-Bac Bui  
Department of Exploration Geology  
Hanoi University of Mining and Geology  
Hanoi  
Vietnam

Anh Ngoc Do  
Department of Underground and Mining  
Construction  
Hanoi University of Mining and Geology  
Hanoi  
Vietnam

Nhat-Duc Hoang  
Faculty of Civil Engineering  
Duy Tan University  
Da Nang  
Vietnam

ISBN 978-3-319-68239-6                      ISBN 978-3-319-68240-2 (eBook)  
<https://doi.org/10.1007/978-3-319-68240-2>

Library of Congress Control Number: 2017956062

© Springer International Publishing AG 2018

This work is subject to copyright. All rights are reserved by the Publisher, whether the whole or part of the material is concerned, specifically the rights of translation, reprinting, reuse of illustrations, recitation, broadcasting, reproduction on microfilms or in any other physical way, and transmission or information storage and retrieval, electronic adaptation, computer software, or by similar or dissimilar methodology now known or hereafter developed.

The use of general descriptive names, registered names, trademarks, service marks, etc. in this publication does not imply, even in the absence of a specific statement, that such names are exempt from the relevant protective laws and regulations and therefore free for general use.

The publisher, the authors and the editors are safe to assume that the advice and information in this book are believed to be true and accurate at the date of publication. Neither the publisher nor the authors or the editors give a warranty, express or implied, with respect to the material contained herein or for any errors or omissions that may have been made. The publisher remains neutral with regard to jurisdictional claims in published maps and institutional affiliations.

Printed on acid-free paper

This Springer imprint is published by Springer Nature  
The registered company is Springer International Publishing AG  
The registered company address is: Gewerbestrasse 11, 6330 Cham, Switzerland

# Preface

We would like to welcome you to International Conference on Geo-spatial Technologies and Earth Resources (GTER-2017), which will be held during October 5–6, 2017, at the Hanoi University of Mining and Geology (HUMG), Hanoi, Vietnam. GTER-2017 is co-organized by HUMG and International Society for Mine Surveying (ISM) to celebrate the 50th anniversary of Department of Mine Surveying (HUMG). The conference is financially supported by Vietnam Mining Science and Technology Association (VMSTA), Vietnam Association of Geodesy, Cartography and Remote Sensing (VGCR), Vietnam National Coal-Mineral Industries Holding Corporation Limited (VINACOMIN), and Dong Bac Corporation (NECO).

The main objective of the conference is to provide a platform for researchers, academicians, and engineers in the field of geospatial technologies and earth resources to present their recent research results. In addition, this conference provides a setting for them to exchange new ideas, innovative thinking, and application experiences face-to-face, to establish research or business relations, and to find partners for future collaboration.

The conference program was organized into three sessions covering topics of geospatial technologies, advance in mining and tunneling, and geological and earth sciences. Overall, the conference has attracted more than 288 papers, and among them, 57 high-quality papers were recommended to submit for this Springer proceedings book for peer-reviewing. Then, the double-blind review process was carried out for the 57 papers, in which each paper has been reviewed for its merit and novelty by at least two reviewers and one editor by matching the content areas. As a result, a total of 24 papers have been finally selected for this book. We believe that this proceedings book provides a broad overview of recent advances in the fields of geospatial technologies and earth resources for readers.

Finally, we would like to express our sincere thanks to (i) the President of ISM : Prof. Anatoly Okhotin; (ii) the Rector of HUMG : Assoc. Prof. Le Hai An; (iii) the Vice Rectors of HUMG : Assoc. Profs. Bui Xuan Nam, Tran Thanh Hai, and Tran Xuan Truong for their help in administrative works and other support. Special thanks go to Michael Leuchner and Bhavana Purushothaman at Springer

International Publishing AG for always responding promptly. We would like to thank all the reviewers for their timely and rigorous reviews of the papers and thank all the authors for their submissions.

October 2017

Dieu Tien Bui  
Anh Ngoc Do  
Hoang-Bac Bui  
Nhat-Duc Hoang

# List of Reviewers

Anh Tuan Nguyen	Hanoi University of Mining and Geology, Vietnam
Ataollah Shirzadi	University of Kurdistan, Iran
Binh Thai Pham	University of Transport Technology, Vietnam
Dinh Hieu Vu	Hanoi University of Mining and Geology, Vietnam
Dinh Sinh Mai	Le Quy Don Technical University, Vietnam
Phuong D. Dao	University of Toronto, Canada
Duc-Anh Nguyen	University College of Southeast Norway, Norway
Haijian Su	China University of Mining and Technology, China
Hanh Hong Tran	Hanoi University of Mining and Geology, Vietnam
Hong-Phuong Nguyen	Vietnam Academy of Science and Technology, Vietnam
Indra Prakash	Bhaskaracharya Institute for Space Applications and Geoinformatics, India
Kien-Trinh Thi Bui	Thuyloi University, Vietnam
Lien T.H Pham	Waikato University, New Zealand
Loi Huy Doan	Institute of Transport Science and Technology, Vietnam
Long Thanh Ngo	Le Quy Don Technical University, Vietnam
Pirat Jaroopattanapong	Chiang Mai University, Thailand
Qian Yin	China University of Mining and Technology, China
Quoc-Phi Nguyen	Hanoi University of Mining and Geology, Vietnam
Quoc-Dinh Nguyen	Vietnam Institute of Geosciences and Mineral Resources
Ryszard Hejmanowski	AGH University of Science and Technology, Poland
Le Hoang Son	VNU University of Science, Hanoi
Tan Manh Do	Hanoi University of Mining and Geology, Vietnam
Thanh-Trung Duong	Hanoi University of Mining and Geology Vietnam
Thanh-Long Nguyen	Vietnam Institute of Geosciences and Mineral Resources
Thu-Trang Le	Hanoi University of Mining and Geology, Vietnam

Tien Dat Pham	University of Tsukuba, Japan
Tran Anh Quang Pham	IRISA/University of Rennes 1, France
Trong Trinh Phan	Vietnam Academy of Science and Technology, Vietnam
Tuan Quoc Vo	Can Tho University, Vietnam
Tuong-Thuy Vu	University of Nottingham, Malaysia
Trung Van Nguyen	Hanoi University of Mining and Geology, Vietnam
Vu Hien Phan	Ho Chi Minh University of Technology, Vietnam



# Contents

<b>A Computational Tool for Time-Series Prediction of Mining-Induced Subsidence Based on Time-Effect Function and Geodetic Monitoring Data</b> . . . . .	1
Nguyen Quoc Long, Xuan-Nam Bui, Luyen Khac Bui, Khoa Dat Vu Huynh, Canh Van Le, Michał Buczek, and Thang Phi Nguyen	
<b>Lightweight Unmanned Aerial Vehicle and Structure-from-Motion Photogrammetry for Generating Digital Surface Model for Open-Pit Coal Mine Area and Its Accuracy Assessment</b> . . . . .	17
Dieu Tien Bui, Nguyen Quoc Long, Xuan-Nam Bui, Viet-Nghia Nguyen, Chung Van Pham, Canh Van Le, Phuong-Thao Thi Ngo, Dung Tien Bui, and Bjørn Kristoffersen	
<b>Energy Analysis in Semiautomatic and Automatic Velocity Estimation for Ground Penetrating Radar Data in Urban Areas: Case Study in Ho Chi Minh City, Vietnam</b> . . . . .	34
Thuan Van Nguyen, Cuong Anh Van Le, Van Thanh Nguyen, Trung Hoai Dang, Triet Minh Vo, and Lieu Nguyen Nhu Vo	
<b>An Integration of Least Squares Support Vector Machines and Firefly Optimization Algorithm for Flood Susceptible Modeling Using GIS</b> . . . . .	52
Viet-Nghia Nguyen, Dieu Tien Bui, Phuong-Thao Thi Ngo, Quoc-Phi Nguyen, Van Cam Nguyen, Nguyen Quoc Long, and Inge Revhaug	
<b>Estimation of Surface Parameters of Tidal Flats Using Sentinel-1A SAR Data in the Northern Coast of Vietnam</b> . . . . .	65
Si Son Tong, Jean Paul Deroin, Thi Lan Pham, and Xuan Cuong Cao	
<b>Reconstruction of Missing Imagery Data Caused by Cloudcover Based on Bayesian Neural Network and Multitemporal Images</b> . . . . .	89
Hien Phu La and Minh Quang Nguyen	

<b>Monitoring Mangrove Forest Changes in Cat Ba Biosphere Reserve Using ALOS PALSAR Imagery and a GIS-Based Support Vector Machine Algorithm</b> . . . . .	103
Tien Dat Pham, Kunihiko Yoshino, and Naoko Kaida	
<b>Detection and Prediction of Urban Expansion of Hanoi Area (Vietnam) Using SPOT-5 Satellite Imagery and Markov Chain Model</b> . . . . .	119
Trung Van Nguyen, Nam Van Nguyen, Ha Thu Thi Le, Hien Phu La, and Dieu Tien Bui	
<b>Analysis of Land Cover Changes in Northern Vietnam Using High Resolution Remote Sensing Data</b> . . . . .	134
Thanh Tung Hoang, Kenlo Nishida Nasahara, and Jin Katagi	
<b>Change Detection in Multitemporal SAR Images Using a Strategy of Multistage Analysis</b> . . . . .	152
Thu Trang Lê, Van Anh Tran, Ha Thai Pham, and Xuan Truong Tran	
<b>Understanding Factors Affecting the Outbreak of Malaria Using Locally-Compensated Ridge Geographically Weighted Regression: Case Study in DakNong, Vietnam</b> . . . . .	166
Tuan-Anh Hoang, Le Hoang Son, Quang-Thanh Bui, and Quoc-Huy Nguyen	
<b>A Novel Hybrid Model of Rotation Forest Based Functional Trees for Landslide Susceptibility Mapping: A Case Study at Kon Tum Province, Vietnam</b> . . . . .	186
Binh Thai Pham, Viet-Tien Nguyen, Van-Liem Ngo, Phan Trong Trinh, Huong Thanh Thi Ngo, and Dieu Tien Bui	
<b>Effects of Residual Soil Characteristics on Rainfall-Induced Shallow Landslides Along Transport Arteries in Bac Kan Province, Vietnam</b> . . .	202
Do Minh Duc, Dao Minh Duc, and Do Minh Ngoc	
<b>Spatial Prediction of Rainfall Induced Shallow Landslides Using Adaptive-Network-Based Fuzzy Inference System and Particle Swarm Optimization: A Case Study at the Uttarakhand Area, India</b> . . . . .	224
Binh Thai Pham and Indra Prakash	
<b>GIS-Based Landslide Spatial Modeling Using Batch-Training Back-propagation Artificial Neural Network: A Study of Model Parameters</b> . . . . .	239
Nhat-Duc Hoang and Dieu Tien Bui	

**A Novel Hybrid Intelligent Approach of Random Subspace Ensemble and Reduced Error Pruning Trees for Landslide Susceptibility Modeling: A Case Study at Mu Cang Chai District, Yen Bai Province, Viet Nam** . . . . . 255  
 Binh Thai Pham and Indra Prakash

**Recent Tectonic Movements Along the Coastal Zone of Tuy Hoa Area (Central Vietnam) and Its Significance for Coastal Hazards in the Case of Sea Level Rise** . . . . . 270  
 Hai Thanh Tran

**Isotopic and Hydrogeochemical Signatures in Evaluating Groundwater Quality in the Coastal Area of the Mekong Delta, Vietnam** . . . . . 293  
 Tran Dang An, Maki Tsujimura, Vo Le Phu, Doan Thu Ha, and Nguyen Van Hai

**Research Progress on Stabilization/Solidification Technique for Remediation of Heavy Metals Contaminated Soil** . . . . . 315  
 Yu Zhang, Cong Lu, Mengyi Xu, Lingling Pan, Nguyen Chau Lan, and Qiang Tang

**Distribution and Reserve Potential of Titanium-Zirconium Heavy Minerals in Quang an Area, Thua Thien Hue Province, Vietnam** . . . . . 326  
 Nguyen Tien Dung, Bui Hoang Bac, Do Manh An, and Tran Thi Van Anh

**Application of Land Subsidence Inversion for Salt Mining-Induced Rock Mass Movement** . . . . . 340  
 Ryszard Hejmanowski and Agnieszka A. Malinowska






**Study on the Coupling Effect Between Surrounding Rock and Support Structures of Tunnels** . . . . . 355  
 Pham Thi Nhan, Guangsheng Zhang, Viet-Nghia Nguyen, and Viet Huy Le

**Numerical Simulation of CFRA Pile Subgrade Reinforcement Based on Recycled Aggregate of Demolition Waste** . . . . . 367  
 Huanda Gu, Cong Lu, Guoqiang Xue, Huilong Wu, Nguyen Chau Lan, and Qiang Tang

**Worthiness Assessment of New Mining Projects: The Case of Potash Mining in Bamnet Narong, Thailand** . . . . . 378  
 Kridtaya Sakamornsnguan and Jürgen Kretschmann

**Author Index** . . . . . 395

# A Computational Tool for Time-Series Prediction of Mining-Induced Subsidence Based on Time-Effect Function and Geodetic Monitoring Data

Nguyen Quoc Long<sup>1</sup> , Xuan-Nam Bui<sup>2</sup> , Luyen Khac Bui<sup>3</sup> ,  
Khoa Dat Vu Huynh<sup>4</sup>, Canh Van Le<sup>1</sup> , Michał Buczek<sup>5</sup> ,  
and Thang Phi Nguyen<sup>1</sup>

<sup>1</sup> Department of Mine Surveying,  
Hanoi University of Mining and Geology, Hanoi, Vietnam  
nguyenquoclong@humg.edu.vn

<sup>2</sup> Department of Surface Mining,  
Hanoi University of Mining and Geology, Hanoi, Vietnam

<sup>3</sup> Department of Geodesy,  
Hanoi University of Mining and Geology, Hanoi, Vietnam

<sup>4</sup> Norwegian Geotechnical Institute (NGI), Oslo, Norway

<sup>5</sup> Department of Engineering Surveying and Civil Engineering,  
AGH University of Science and Technology, Kraków, Poland

**Abstract.** Underground mining-induced land subsidence may cause serious damage to engineering structures (e.g., buildings or roads) therefore, it is necessary to predict the subsidence with the highest possible accuracy. This paper proposes a new method for estimating preliminary values of the parameters to the modified Knothe time function, resulting in an improved capability of predicting land subsidence. A computational tool incorporating the proposed method has been developed to practically and numerically facilitate the time-series prediction of mining subsidence. A case study at the Mong Duong colliery at Quang Ninh province in Vietnam was considered and back-analyzed to validate the capability and accuracy of the tool. The accuracy of the subsidence prediction was evaluated using Root Mean Square Errors (*RMSE*), Mean Absolute Errors (*MAE*), and the Correlation coefficient (*r*). The result showed that the proposed method predicted reasonably well both the calibrating dataset (*RMSE* = 15 mm, *MAE* = 13 mm, *r* = 0.996) and the validating dataset (*RMSE* = 44 mm, *MAE* = 37 mm, *r* = 0.857). Based on the comparison results, it is concluded that the developed tool incorporating the proposed method is suitable for predicting underground mining-induced land subsidence.

**Keywords:** Computational tool · Time-series prediction · Modified knothe time function · Underground mining · Geodetic monitoring

## 1 Introduction

The rapid growths in the world's population and economy have resulted in continuous increase in energy and mineral consumption. To meet this high demand for minerals, mining activities have continuously and rapidly expanded over time, all over the world. Underground coal mining can cause serious damages, as a result of mining-induced land subsidence, to engineering structures such as buildings, roads, railways, and drainage systems [1–3]. It is important to note that mining-induced land subsidence can occur not only during active mining but also several decades after the completion of active mining. In Vietnam, damage caused by mine surface deformation is commonly observed and occurs in most of all underground mining areas, especially at the Quang Ninh coal basin [4]. For example, in 1991 mining-induced subsidence caused huge damage to the road at the Deo Nai mine [5]. In 2000, a subsidence observed at the Mao Khe coal mine caused serious damage for the fan station [4]. Several residential houses were heavily damaged and the 110 kV electricity line was destroyed because of a subsidence at the Mong Duong colliery [6, 7]. It is concluded that one of the main reasons of causing the above land subsidence phenomena in Vietnam was the lack of practical and sophisticated methods for accurately predicting mining-induced land subsidence.

Many methods have been developed and continuously improved to better predict and estimate land subsidence due to mining activities [1, 8, 9]. According to Bahuguna, et al. [10], subsidence prediction methods can be basically classified into three categories: empirical techniques, influence function and theoretical modelling. Among them, the Knothe time function (KTF) is considered to be the most effective and widely used [11, 12]. The major advantage of the KTF method is that it can describe the process of surface subsidence in time through a set of differential mathematical equations [13, 14]. By using the KTF method, land subsidence over time due to underground mining activity can be simply predicted through a subsidence curve. However, land subsidence is generally a complex and nonlinear process so that the application of the original KTF method is not able to correctly capture the whole process of surface subsidence. Wang [15] reported that the prediction accuracy of the KTF models could be low in many cases. Therefore, some modifications of KTF have been proposed [16–18], i.e. a modified function adding a constant parameter to the KTF [19]. Although many recent modified KTF models have made it possible to accurately predict land subsidence over time, it is still difficult and time-consuming to properly determine the function parameters due to the fact that these parameters heavily depend on the estimation of their preliminary values [19]. Therefore, research works are still needed to further improve the prediction accuracy of mining-induced land subsidence.

This research addresses the aforementioned limitation by proposing a new method for estimating the preliminary parameter values of the modified KTF model proposed by Chinh [19], leading to an improved capability of predicting land-surface subsidence. The proposed method was further used to develop a computational tool for time-series prediction of mining subsidence. It is noted that the computational tool was developed using Visual C.net programming language. A case study of the Mong Duong colliery at Quang Ninh province in Vietnam was considered to validate both the current model and the computational tool. The geodetic time-series data of mining subsidence

measured from 2013 to 2015 with 12 epochs were used as input to the modified KTF model. The subsidence prediction accuracy was assessed using Root Mean Square Error (*RMSE*), Mean Absolute Error (*MAE*), and the Correlation coefficient (*r*).

## 2 Methodology

### 2.1 Knothe Time Function and Its Modified Version

According to Knothe [13, 14], the relationship between a time parameter and land subsidence can be established using the following equation:

$$\frac{d\eta(t)}{dt} = b[\eta_{max} - \eta(t)] \quad (1)$$

where  $b$  is a parameter describing the influence of geological and mining conditions on the subsidence progress with time;  $\eta_{max}$  and  $\eta(t)$  are the final subsidence and the subsidence at the time  $t$ , respectively.

By integrating Eq. 1 with respect to  $t$ , the KTF model for surface dynamic subsidence could be written as below:

$$\eta^p(t_i) = \eta_{max} \cdot [1 - e^{-bt_i}] \quad (2)$$

It is observed from Eq. 2 that there is only one parameter  $b$  which plays a significant role in predicting surface subsidence. This limitation could result in low prediction accuracy when using the KTF model in many cases [15]. To improve the prediction, Chinh [19] proposed a modified KTF model described as follows:

$$\eta^p(t_i) = \eta_{max} \left[ 1 - e^{-b(t_i)^c} \right] \quad (3)$$

where  $\eta^p(t_i)$  is the predicted subsidence of the  $i^{\text{th}}$  epoch;  $c$  is the fitting parameter.

Literature review indicates that the preliminary value of  $c$  equal to 2 is commonly assumed in various works [19]. The uncertainty in defining the fitting parameter  $c$  may result in large errors in some complex land subsidence. In some cases, it is even impossible to find  $c$  in a given dataset. Thus, the approach used for estimating the preliminary  $c$ -value needs to be improved in order to better determine the parameter  $c$ .

### 2.2 Method for Determination of Preliminary Parameters

From Eq. 3, the relation between  $\eta^p(t_i)$  and the measured value  $\eta(t_i)$  can be derived as:

$$\eta^p(t_i) = \eta(t_i) + V_{\eta(t_i)} \quad (4)$$

where  $V_{\eta(t_i)}$  is residual value at the time  $t_i$ . The model parameters  $\eta_{max}$ ,  $b$ ,  $c$  are determined based on the least-squares principle using the following equations:

$$\begin{cases} \eta_{max} = \eta_{max}^0 + \delta\eta_{max} \\ b = b^0 + \delta b \\ c = c^0 + \delta c \end{cases} \quad (5)$$

where  $\eta_{max}^0, b^0, c^0$  are the preliminary values of the modified KTF;  $\delta\eta_{max}, \delta b, \delta c$  are the residual ones.

Based on Eq. 4 and the system of Eq. 5, the residual equation can be rewritten as follows:

$$V_{\eta(t_i)} = \eta^p(t_i)(\eta_{max}^0 + \delta\eta_{max}, b^0 + \delta b, c^0 + \delta c) - \eta(t_i) \quad (6)$$

To estimate preliminary values for  $\eta_{max}^0, b^0, c^0$ , the following steps are proposed: Rewriting Eq. 3 as follows:

$$1 - \frac{\eta(t_i)}{\eta_{max}^0} = e^{-b^0(t_i)c^0} \quad (7)$$

By taking the natural logarithm of the both sides of Eq. 7, the modified KTF model will become:

$$\ln \left[ 1 - \frac{\eta(t_i)}{\eta_{max}^0} \right] = -b^0(t_i)c^0 = \ln \left[ 1 - \frac{\eta(t_i)}{\eta_{max}^0} \right] \quad (8)$$

At the  $(i+1)^{th}$  epoch, Eq. 8 is formed as:

$$(t_{i+1})c^0 = \frac{\ln \left[ 1 - \frac{\eta(t_{i+1})}{\eta_{max}^0} \right]}{-b^0} \quad (9)$$

Dividing Eqs. 8 and 9 gives the following equation for estimating preliminary parameter  $c^0$ :

$$c^0 = \log_{\frac{t_i}{t_{i+1}}} \left[ \frac{\ln \left[ 1 - \frac{\eta(t_i)}{\eta_{max}^0} \right]}{\ln \left[ 1 - \frac{\eta(t_{i+1})}{\eta_{max}^0} \right]} \right] \quad (10)$$

The value  $c^0$  from Eq. 10 is substituted into Eq. (8), then  $b^0$  can be determined as follows:

$$b^0 = -\frac{\ln \left[ 1 - \frac{\eta(t_i)}{\eta_{max}^0} \right]}{(t_i)c^0} \quad (11)$$

### 2.3 Computation of Modified KTF Parameters

If the preliminary parameters are estimated sufficiently close to their desired values then the residuals are small. In this case, the residual value  $V_{\eta(t_i)}$  in Eq. 4 can be approximated by a Taylor series expansion, retaining only the first order terms of  $\partial_{\eta_{max}}$ ,  $\delta_b$ ,  $\delta_c$  as follows:

$$V_{\eta(t_i)} = \eta^p(t_i)(\eta_{max}^0, b^0, c^0) + \left(\frac{\partial\eta^p(t_i)}{\partial\eta_{max}}\right)_0 \delta_{\eta_{max}} + \left(\frac{\partial\eta^p(t_i)}{\partial b}\right)_0 \delta_b + \left(\frac{\partial\eta^p(t_i)}{\partial c}\right)_0 \delta_c - \eta(t_i) \quad (12)$$

where  $\frac{\partial\eta^p(t_i)}{\partial\eta_{max}} = 1 - e^{-b^0(t_i)^{c^0}}$ ;  $\frac{\partial\eta^p(t_i)}{\partial b} = \eta_{max}(t_i)^{c^0} e^{-b^0(t_i)^{c^0}}$ ;  
and  $\frac{\partial\eta^p(t_i)}{\partial c} = \eta_{max} b^0 \cdot e^{-b^0(t_i)^{c^0}} (t_i)^{c^0} \ln(t_i)$

The residual between the predicted values and their corresponding measured values is expressed as follows:

$$\ell_i = \eta^p(t_i)(\eta_{max}^0, b^0, c^0) - \eta(t_i) \quad (13)$$

Finally, the observation equation is derived as:

$$V_{\eta(t_i)} = \left(\frac{\partial\eta^p(t_i)}{\partial\eta_{max}}\right)_0 \delta_{\eta_{max}} + \left(\frac{\partial\eta^p(t_i)}{\partial b}\right)_0 \delta_b + \left(\frac{\partial\eta^p(t_i)}{\partial c}\right)_0 \delta_c + \ell_i \quad (14)$$

The coefficients of Eq. 14 are symbolized as  $\left(\frac{\partial\eta^p(t_i)}{\partial\eta_{max}, b, c}\right)_0 = a_{ij}$ , with  $i = 1 \div n$  and  $j = 1, 2, 3$ , corresponding to the unknowns  $\partial_{\eta_{max}}$ ,  $\delta_b$ ,  $\delta_c$ . By doing so, a system of linear equations in Eq. 14 can be represented in matrix form as follows:

$$\mathbf{V} = \mathbf{A} \cdot \mathbf{X} + \mathbf{L} \quad (15)$$

where  $\mathbf{A}$  is the design matrix,  $\mathbf{V}$  is the vector of discrepancies,  $\mathbf{L}$  is the vector of observations, and  $\mathbf{X}$  is the vector of unknowns.

$$\mathbf{A} = \begin{bmatrix} a_{1,1} & a_{1,2} & a_{1,3} \\ a_{2,1} & a_{2,2} & a_{2,3} \\ \dots & \dots & \dots \\ a_{n,1} & a_{n,2} & a_{n,3} \end{bmatrix}; \mathbf{V} = \begin{bmatrix} V_1 \\ V_2 \\ \dots \\ V_n \end{bmatrix}; \mathbf{L} = \begin{bmatrix} \ell_1 \\ \ell_2 \\ \dots \\ \ell_n \end{bmatrix}; \mathbf{X} = \begin{bmatrix} \partial_{\eta_{max}} \\ \delta_b \\ \delta_c \end{bmatrix}. \quad (16)$$

The following normal equation can be derived from a set of different observation equations:

$$(\mathbf{A}^T \mathbf{A}) \mathbf{X} + (\mathbf{A}^T \mathbf{L}) = 0 \quad (17)$$

$$\mathbf{X} = -(\mathbf{A}^T \mathbf{A})^{-1} \mathbf{A}^T \mathbf{L} \quad (18)$$



Considering these derived  $X$  values, parameters  $\eta_{max}$ ,  $b$ ,  $c$  of the prediction model can be firstly determined by Eq. 5, and then Eq. 3 is used to calculate the subsidence value of the  $i^{\text{th}}$  epoch.

## 2.4 Accuracy Assessment

Accuracy of the current prediction model is assessed by comparing the predicted result with the measured data in terms of Root Mean Square Error ( $RMSE$ ), mean absolute error ( $MAE$ ) and correlation coefficient ( $r$ ). The lower  $RMSE$  and  $MAE$  together with the higher  $r$  indicate the more accurate prediction of the model. More specifically, the following equations are used:

$$RMSE = \sqrt{\frac{1}{n} \sum_{i=1}^n [\eta^p(t_i) - \eta(t_i)]^2} \quad (19)$$

$$MAE = \frac{1}{n} \sum_{i=1}^n |\eta(t_i) - \eta^p(t_i)| \quad (20)$$

$$r = \frac{\sum_{i=1}^n (\eta(t_i) - \bar{\eta})(\eta^p(t_i) - \bar{\eta}^p)}{\sqrt{\sum_{i=1}^n (\eta(t_i) - \bar{\eta})^2 * \sum_{i=1}^n (\eta^p(t_i) - \bar{\eta}^p)^2}} \quad (21)$$

where  $\eta(t_i)$  and  $\eta^p(t_i)$  are the measured and the predicted values at  $t_i$ ;  $\bar{\eta}$  and  $\bar{\eta}^p$  are the corresponding medium values of measured and predicted values, respectively.

## 3 Computational Tool for Time-Series Prediction of Mining Subsidence

Based on the modified KTF method proposed in the Sect. 2, a computational tool for time-series prediction of mining subsidence was developed. It is noted that the tool was programmed in Visual Studio.Net 2013 Ultimate, an object-oriented programming language with Visual Studio DevExpress Universal 15.2.7 library package [20]. The tool can run in different versions of Microsoft Windows including the version 7, 8 and 10 and it is also compatible with both 32- and 64-bit environments.

Figure 1 presents a workflow for the determination of the preliminary parameters ( $\eta_{max}^0, b^0, c^0$ ) of the modified KTF method. A workflow for the computation of the corresponding final parameters ( $\eta_{max}, b, c$ ) based on the least-squares principle and accuracy assessment ( $RMSE$ ,  $MAE$  and  $r$ ) is illustrated in Fig. 2.

A Graphic User Interface (GUI) of the computational tool is shown in Fig. 3. Input data could be either entered directly through the GUI or imported from text or excel files. The computed results including the model's parameters and the predicted values, are stored both in txt and csv formats, which make them easier to be shared with and edited by other softwares. Furthermore, measurement data and prediction results can be exported/converted into a graphical file in Drawing Exchange Format (DXF). DXF is a

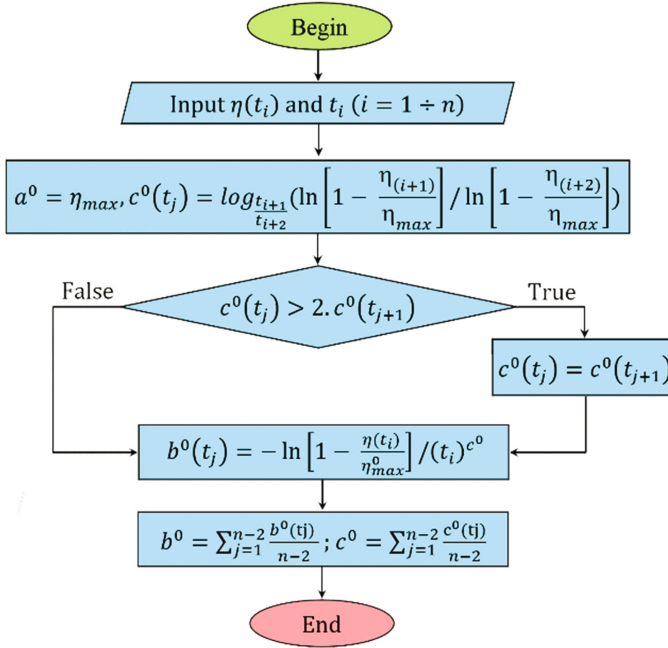


**Fig. 1.** Workflow used for estimating preliminary parameters of modified KTF

CAD data file format developed by Autodesk for enabling data interoperability between AutoCAD and other programs [21].

## 4 A Case Study of Mining Subsidence at Mong Duong Colliery, Quang Ninh Province in Vietnam

### 4.1 Description of the Study Site

Mong Duong colliery, a typical coal mine in Vietnam with more than 35-year operation, is selected as a case study for validating the modified KTF model. This mine is located about 10 km north of Cam Pha city, as shown in Fig. 4. The mine boundary was taken according to the Decision No. 1122/QD-HDQT dated on May 16, 2008, by the Chairman of the Vinacomin's Board of Directors on Approving the master plan for coal mines boundary of the Vietnam National Coal - Mineral Industries Holding Corporation Limited.

From explorations' results, there are in total 22 coal seams in the Mong Duong colliery. To date, the coal is excavated in various seams and multi-layer seams, mainly varying from  $-100$  m to  $-250$  m below the sea level. They consist of seams H10, G9 in the East Wing, G9 in the West Wing, G9 in Vu Mon area, II (11) and K8, etc. There are two shafts including the main shaft and the auxiliary shaft, which were built correspondingly from  $+18$  m and  $+6.5$  m down to  $-97.5$  m.

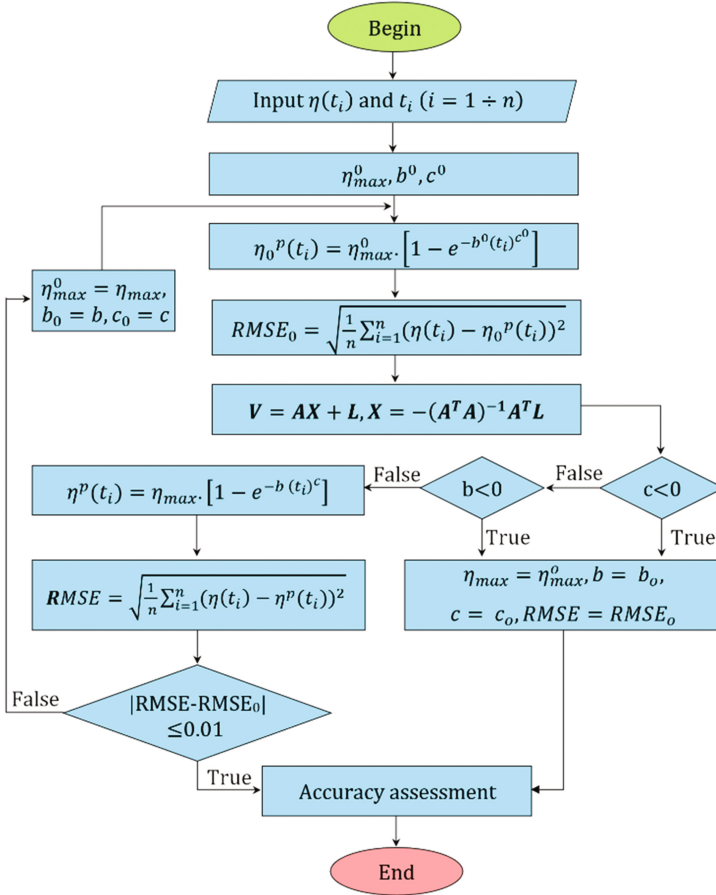


Fig. 2. Workflow used for the computing final parameters of modified KTF

Underground mining activity in the Mong Duong colliery has resulted in various subsidence problems that caused several damages to residential areas, the main shaft, the wind turbine station, the 110/35/6 kV substation and office buildings on the mine surface.

#### 4.2 Data Collection and Processing

To assess and forecast potential land subsidence due to the underground mining at the Mong Duong colliery, a monitoring network has been established in the G9 BMD seam, where the Face No.2 was mined. The G9 BMD seam has an average thickness of 2.5 m with an average slope angle of 35°. The Face No.2 was commenced in the second quarter 2013 and finished in second quarter 2014. The panel was prepared along the seam strike and retreated, cutting coal by blasting and supporting the roof using hydraulic props (Fig. 5).

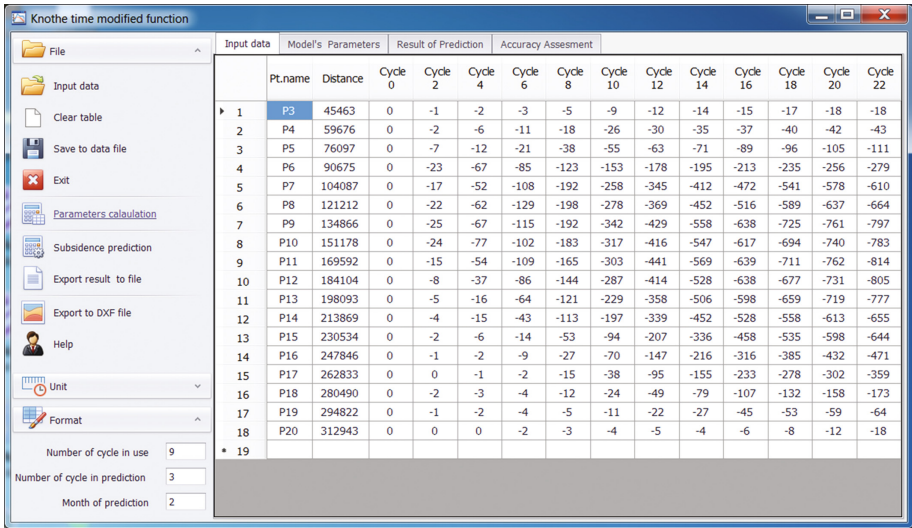


Fig. 3. Illustration of Graphic User Interface of computational tool

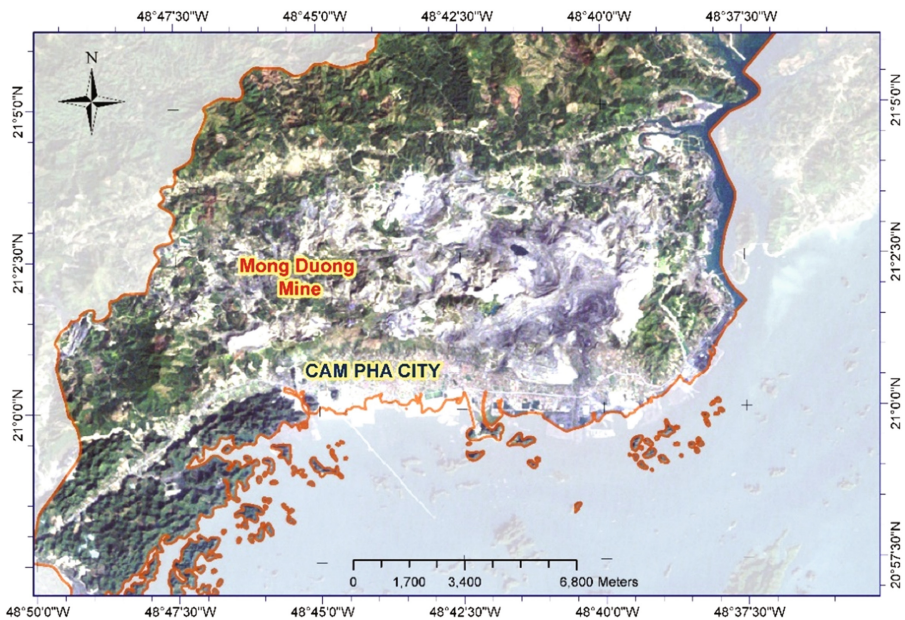


Fig. 4. Mong Dong colliery location

The measurements were carried out using Leica NAK2 automatic level instrument shown in Fig. 6. The observation network consists of 2 leveling lines - the line P was established in the strike direction and the line D is along the dip direction of the Face



**Fig. 5.** Face No.2 with hydraulic props (photo courtesy of Long Quoc Nguyen)



**Fig. 6.** Leica NAK2 level

No.2, as illustrated in Fig. 7. The land subsidence data have been continuously measured from 2013 to 2015 with 12 repeated epochs. The time interval between two successive epochs is approximately 2 months. Measurement precision satisfied the Vietnam National Specifications on Mine Surveying (closed loop misclosure is less than  $20\sqrt{L}(\text{mm})$  [22] with  $L$  is the total length of the leveling route.

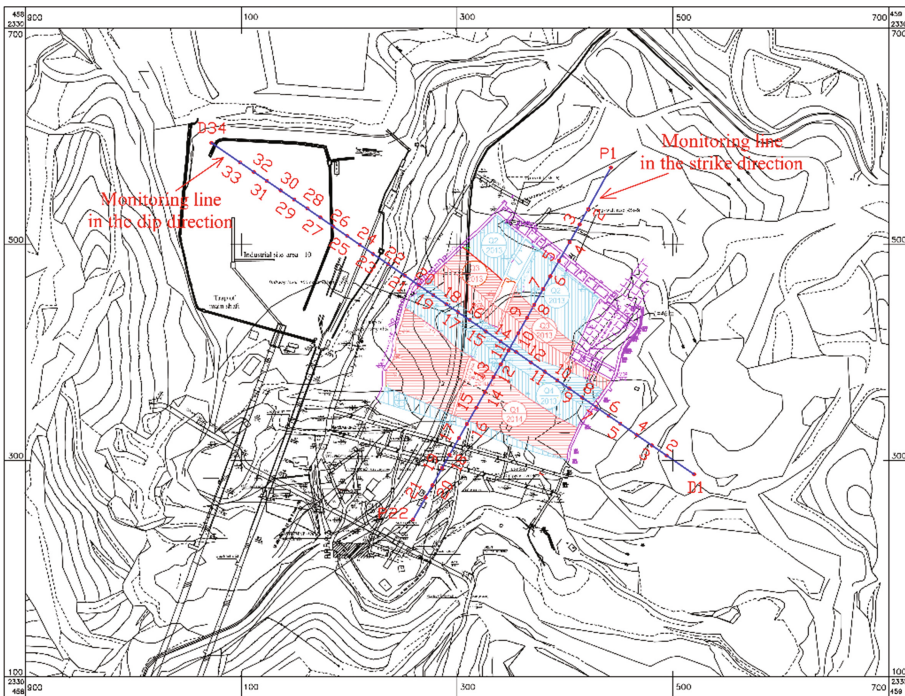


**Fig. 7.** The monitoring lines at the G9 BMD seam of the Mong Duong colliery

In order to detect and eliminate outliers, the difference in level between two adjacent benchmarks is determined from both forward and backward measurements. The difference in level between benchmarks is then taken equal to the average of the two values.

The monitoring observation results obtained from 16 benchmarks on the line P (see Fig. 7) were considered in the evaluation of the suitability of the algorithm used for determining the model parameters as well as the prediction accuracy of the modified KTF model. The datasets are summarized in Table 1.

**Table 1.** Measured subsidence (mm) with time from 16 benchmarks on line P

Point name	Cycle											
	1	2	3	4	5	6	7	8	9	10	11	12
P3	0	-1	-2	-3	-5	-9	-12	-14	-15	-17	-18	-18
P4	0	-2	-6	-11	-18	-26	-30	-35	-37	-40	-42	-43
P5	0	-7	-12	-21	-38	-55	-63	-71	-89	-96	-105	-111
P6	0	-23	-67	-85	-123	-153	-178	-195	-213	-235	-256	-279
P7	0	-17	-52	-108	-192	-258	-345	-412	-472	-541	-578	-610
P8	0	-22	-62	-129	-198	-278	-369	-452	-516	-589	-637	-664
P9	0	-25	-67	-115	-192	-342	-429	-558	-638	-725	-761	-797
P10	0	-24	-77	-102	-183	-317	-416	-547	-617	-694	-740	-783
P11	0	-15	-54	-109	-165	-303	-441	-569	-639	-711	-762	-814
P12	0	-8	-37	-86	-144	-287	-414	-528	-638	-677	-731	-805
P13	0	-5	-16	-64	-121	-229	-358	-506	-598	-659	-719	-777
P14	0	-4	-15	-43	-113	-197	-339	-452	-528	-558	-613	-655
P15	0	-2	-6	-14	-53	-94	-207	-336	-458	-535	-598	-644
P16	0	-1	-2	-9	-27	-70	-147	-216	-316	-385	-432	-471
P17	0	0	-1	-2	-15	-38	-95	-155	-233	-278	-302	-359
P18	0	-2	-3	-4	-12	-24	-49	-79	-107	-132	-158	-173

### 4.3 Land Subsidence Model and Its Performance Assessment

The data in the first nine cycles of 16 points were used to calibrate the subsidence model, whereas the remaining data (i.e. the data of cycles 10, 11 and 12) were used for validating the model as well as confirming its predictive capability. The algorithm described in Sect. 2 was applied to determine the parameters of the subsidence model for each point for the first 9 cycles. The calculated parameters are given in Fig. 8. The results show that the model performs well with the determining parameters set.

In this study, the authors did not use observation points such as points 1, point 2, point 19, and point 20 either to build the prediction model or to evaluate prediction results. As those points lying at the beginning and at the ending of monitoring lines, their settlement rules are not stable, hence, their subsidence curves do not match the curve for the modified KTF model.

To validate the predictive ability of the model, these calculated parameters have been used to predict the subsidence of points at the remaining cycles, i.e., the 10<sup>th</sup>, 11<sup>th</sup> and 12<sup>th</sup> cycles. The subsidence calculated from the model was subsequently compared

Input data	Model's Parameters	Result of Prediction	Accuracy Assessment				
	Point name	$\eta_{max}$	b	c	RMSE (mm)	MAE (mm)	r
1	P3	-16,378	2,648	2,604	0	0	0,997
2	P4	-40,305	2,572	2,067	1	0	0,999
3	P5	-134,787	1,030	1,673	3	2	0,996
4	P6	-281,385	1,421	1,297	4	3	0,999
5	P7	-624,896	1,409	2,003	4	3	1,000
6	P8	-822,095	1,000	1,833	4	3	1,000
7	P9	-1031,594	1,022	2,145	12	10	0,999
8	P10	-867,376	1,279	2,269	15	13	0,998
9	P11	-776,726	1,796	2,694	14	11	0,998
10	P12	-722,038	1,945	2,917	9	6	0,999
11	P13	-730,788	1,739	3,219	6	5	1,000
12	P14	-586,518	2,337	3,545	5	4	1,000
13	P15	-601,833	1,437	4,298	5	4	0,999
14	P16	-476,517	1,077	4,000	4	3	0,999
15	P17	-326,077	1,246	4,713	3	2	1,000
16	P18	-144,227	1,361	4,129	1	1	1,000
** 17							

Fig. 8. Model parameters and its accuracy

with that of observations with a deviation between predicted and monitoring data calculated by Eq. 22.

$$\Delta_i = \eta_i - \eta'_i \tag{22}$$

where  $\Delta_i$  is the difference between predicted value and its respective measurement of the  $i^{th}$  point;  $\eta_i$  is the subsidence calculated from measurement data and  $\eta'_i$  is the value of prediction.

Small deviations shown in (Fig. 9) confirm a good model obtained. The biggest errors in prediction is at the point P9 with predicted errors at epochs 10, 11, 12 are

Input data	Model's Parameters	Result of Prediction	Accuracy Assessment							
	Point name	Cycle 18 ( $\eta_{18}$ )	Cycle 18 ( $\eta'_{18}$ )	$\Delta_{18}$	Cycle 20 ( $\eta_{20}$ )	Cycle 20 ( $\eta'_{20}$ )	$\Delta_{20}$	Cycle 22 ( $\eta_{22}$ )	Cycle 22 ( $\eta'_{22}$ )	$\Delta_{22}$
1	P3	-16	-17	1	-16	-18	2	-16	-18	2
2	P4	-39	-40	1	-40	-42	2	-40	-43	3
3	P5	-96	-96	0	-105	-105	0	-111	-111	0
4	P6	-228	-235	7	-239	-256	17	-249	-279	30
5	P7	-520	-541	21	-556	-578	22	-581	-610	29
6	P8	-584	-589	5	-640	-637	-3	-685	-664	-21
7	P9	-755	-725	-30	-833	-761	-72	-895	-797	-98
8	P10	-704	-694	-10	-763	-740	-23	-805	-783	-22
9	P11	-711	-711	0	-747	-762	15	-765	-814	49
10	P12	-676	-677	1	-705	-731	26	-717	-805	88
11	P13	-673	-659	-14	-710	-719	9	-725	-777	52
12	P14	-570	-558	-12	-583	-613	30	-586	-655	69
13	P15	-546	-535	-11	-588	-598	10	-600	-644	44
14	P16	-392	-385	-7	-442	-432	-10	-466	-471	5
15	P17	-289	-278	-11	-317	-302	-15	-325	-359	34
16	P18	-128	-132	4	-140	-158	18	-143	-173	30
** 17										

Fig. 9. Differences between measured and predicted values

Input data	Model's Parameters	Result of Prediction	Accuracy Assessment			
	Point name	RMSE (mm)	MAE (mm)	RMSE/Smax (%)	MAE/Smax (%)	r
1	P3	2	1	9	9	0,969
2	P4	2	2	6	5	1,000
3	P5	0	0	0	0	0,998
4	P6	21	18	7	6	0,996
5	P7	24	24	4	4	0,998
6	P8	13	9	2	1	0,994
7	P9	73	67	7	6	0,998
8	P10	20	19	2	2	0,997
9	P11	29	21	4	3	0,980
10	P12	53	39	7	5	0,948
11	P13	32	25	4	3	0,973
12	P14	44	37	7	6	0,962
13	P15	27	22	4	4	0,977
14	P16	7	7	2	1	0,989
15	P17	22	20	7	6	0,857
16	P18	20	17	14	12	0,993
17						

Fig. 10. Assessment of predicted results

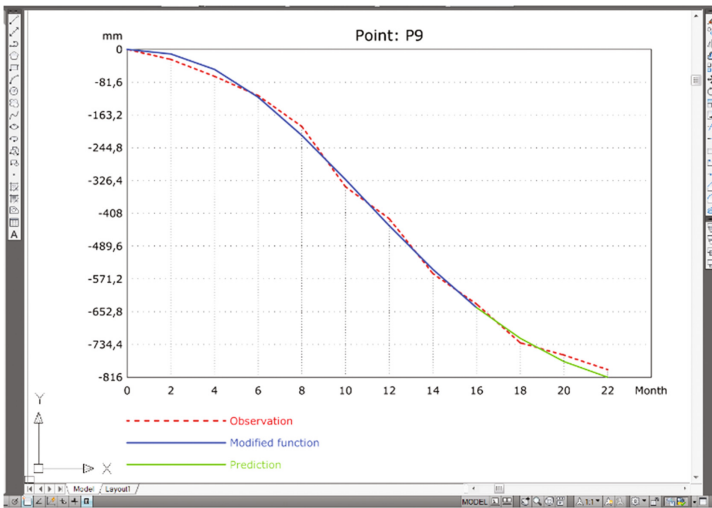
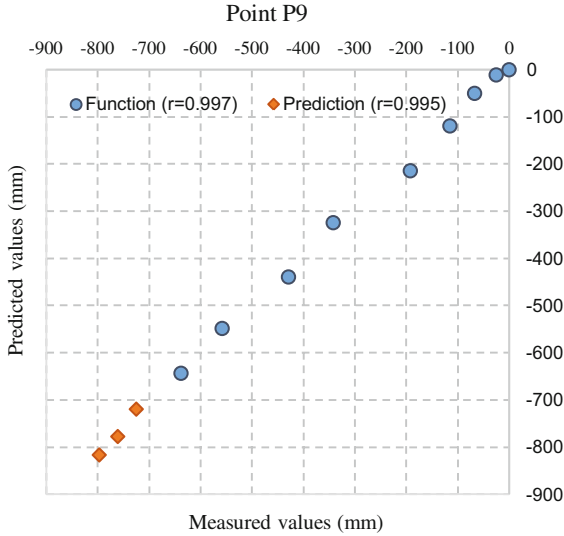


Fig. 11. Comparison of prediction and observation curves of point P9

-30 mm, -72 mm and -98 mm, respectively. These errors correspond to 4%, 8.6%, 11% of the actual subsidence magnitude of the corresponding measurement epochs. These errors are proportional to the temporal separation between the time of prediction and that of the last stage used for building prediction model, i.e., the 9<sup>th</sup> epoch. More strictly, the longer the temporal separation is, the higher error in prediction we get.

Statistical indicators including  $RMSE$ ,  $MAE$ ,  $RMSE/\eta_{max}$ ,  $MAE/\eta_{max}$  and  $r$  were used to assess the accuracy of the modified KTF model in predicting subsidence





**Fig. 12.** Correlation between the measured and predicted values of point P9

monitored along the considered line P. The validation dataset is given in Fig. 10. It can be seen from the calculated results that the largest *RMSE* and *MAE* values are 44 mm and 37 mm, respectively, which are actually equivalent to 7% and 6% of maximum subsidence. The largest  $RMS/\eta_{\max}$  and  $RMS/\eta_{\max}$  values are obtained at point P18, which equal to 14% and 12%, respectively. This can be explained by the fact that this point is close to the trough subsidence edge so that the rule of point settlement has not been well-defined.

Figure 11 plots a comparison of the anticipated curve of point P9, which is calculated from Eq. (3), with the curve of actual values. It is seen from the figure that the model is able to predict very well the surface subsidence curve observed in the Mong Duong colliery.

The correlation coefficients between predicted and measured values for both cases of parameters determination and subsidence prediction are plotted in Fig. 12. With high values in the building model and the prediction results, it indicates that the predictive model is consistent with the measured data.

## 5 Conclusion

This research proposes a new method for calculating the preliminary values of the input parameters of the modified KTF model proposed by Chinh [19]. The method is basically based on the least-squares principle and observation data, which results in a more practical facilitation to the determination of model parameters. The computational tool has been developed incorporating a friendly user-interface and more flexibility for post-processing of the calculated results.

The functionality and accuracy of the tool were evaluated and validated against the measured subsidence values at 16 monitoring points along the observation line P which is located in the Face. No.2 at the Mong Duong colliery. The comparison result shows a very well agreement between the model prediction values and their corresponding geodetic monitoring data, where the largest *RMSE* and *MAE* are 44 mm and 37 mm, respectively. The smallest correlation coefficient *r* is calculated equal to 0.857, which indicates a high correlation between the monitoring measurements and their predicted values. It is concluded that the developed tool incorporating the modified KTF model is useful and suitable for predicting and evaluating potential mining-induced subsidence in the mining industry. Thereby, the tool can support appropriate strategy to prevent and minimize potential impact caused by land subsidence phenomenon.

A main limitation of this research work is that points lying at the beginning and at the end of the observation line have been excluded from the calculation model as they could have influenced by an irregular process of subsidence. The modified KTF applied in this research, therefore, cannot represent the subsidence of these points over time. More flexible prediction models are thus necessary.

**Acknowledgement.** This research was funded by the Mong Duong coal joint stock company and the Department of Mine Surveying, Hanoi University of Mining and Geology. The funding support is greatly appreciated.

**Conflict of interest.** The authors declare that there is no conflict of interest.

## References

1. Reddish, D., Whittaker, B.: *Subsidence: Occurrence, Prediction and Control*. Elsevier, New York (1989)
2. Can, E., Kuşcu, Ş., Kartal, M.E.: Effects of mining subsidence on masonry buildings in Zonguldak hard coal region in Turkey. *Environ. Earth Sci.* **66**, 2503–2518 (2012)
3. Bozeman, M.: *Underground Hard-Rock Mining: Subsidence and Hydrologic Environmental Impacts*. Google Scholar (2002)
4. Phung, D.M.: *Selection of Appropriate Technical and Technological Solutions for Exploitation in Areas Where Existing Historical, Cultural, Industrial and Civil Works*. Vinacomin (2011)
5. Truc, K.K.: *Defining land subsidence parameters of Thongnhat coal mine*. Institute of Mining Science and Technology (1991)
6. Long, Q.N.: Sectional diagram of dynamic subsidence trough at the Mong Duong coal mine: evaluation and prediction. *J. Min. Earth Sci. (JMES)* **56**, 58–66 (2016)
7. Long, Q.N., My, C.V., Luyen, K.B.: Divergency verification of predicted values and monitored deformation indicators in specific condition of Thong Nhat underground coal mine (Vietnam). *Geoinf. Pol.* **15**, 15–22 (2016)
8. Jarosz, A., Karmis, M., Sroka, A.: Subsidence development with time—experiences from longwall operations in the appalachian coalfield. *Geotech. Geol. Eng.* **8**, 261–273 (1990)
9. Liu, X., Wang, J., Guo, J., Yuan, H., Li, P.: Time function of surface subsidence based on Harris model in mined-out area. *Int. J. Min. Sci. Technol.* **23**, 245–248 (2013)
10. Bahuguna, P., Srivastava, A., Saxena, N.: A critical review of mine subsidence prediction methods. *Min. Sci. Technol.* **13**, 369–382 (1991)

11. Hu, Q.F., Cui, X.M., Wang, G., Wang, M.R., Ji, Y.X., Xue, W.: Key technology of predicting dynamic surface subsidence based on Knothe time function. *JSW* **6**, 1273–1280 (2011)
12. Zhang, Z., Zou, Y., Chen, J., Wang, Y.: Prediction model of land dynamic settlement in coal mining subsidence area. *Trans. Chin. Soc. Agric. Eng.* **32**, 246–251 (2016)
13. Lian, X.: Prediction model of dynamic subsidence caused by underground coal mining. *Electron. J. Geotech. Eng.* **21** (2016)
14. Hu, Q., Deng, X., Feng, R., Li, C., Wang, X., Jiang, T.: Model for calculating the parameter of the Knothe time function based on angle of full subsidence. *Int. J. Rock Mech. Min. Sci.*, 19–26 (2015)
15. Wang, C.: Analysis on the improved time function model of surface subsidence. *Electron. J. Geotech. Eng.* **19** (2015)
16. Zhanqiang, C., Jinzhuang, W.: Study on the time function of surface subsidence - The Improved Knothe time function. *Chin. J. Rock Mechan. Eng.* **9**, 018 (2003)
17. Cui, X., Miao, X., Wang, J.A., Yang, S., Liu, H., Song, Y., Liu, H., Hu, X.: Improved prediction of differential subsidence caused by underground mining. *Int. J. Rock Mech. Min. Sci.* **37**, 615–627 (2000)
18. Han, H.L., Cui, B.: Modeling of surface subsidence based on time function. *Adv. Mater. Res.* **422**, 318–321 (2012)
19. Chinh, N.D.: *Geodetic Methods for Geodynamics*. Hanoi University of Mining and Geology, Hanoi (2003)
20. <https://www.devexpress.com/>
21. [https://www.autodesk.com/techpubs/autocad/acadr14/dxf/dxf\\_reference.htm](https://www.autodesk.com/techpubs/autocad/acadr14/dxf/dxf_reference.htm)
22. Ministry of Information & Communications: *Vietnam National Specifications on Mine Surveying*, Vietnam (2015)

# Lightweight Unmanned Aerial Vehicle and Structure-from-Motion Photogrammetry for Generating Digital Surface Model for Open-Pit Coal Mine Area and Its Accuracy Assessment

Dieu Tien Bui<sup>1</sup>(✉), Nguyen Quoc Long<sup>2</sup>, Xuan-Nam Bui<sup>3</sup>,  
Viet-Nghia Nguyen<sup>2</sup>, Chung Van Pham<sup>2</sup>, Canh Van Le<sup>2</sup>,  
Phuong-Thao Thi Ngo<sup>4</sup>, Dung Tien Bui<sup>5</sup>, and Bjørn Kristoffersen<sup>1</sup>

<sup>1</sup> GIS and IT Group, Department of Business and IT,  
University College of Southeast Norway,  
Gullbringvegen 36, 3800 Bø i Telemark, Norway  
Dieu. T. Bui@usn.no

<sup>2</sup> Department of Mine Surveying,  
Hanoi University of Mining and Geology, Hanoi, Vietnam  
Nguyenquoclong@humg.edu.vn

<sup>3</sup> Faculty of Mining, Hanoi University of Mining and Geology, Hanoi, Vietnam  
Buixuannam@humg.edu.vn

<sup>4</sup> Faculty of Information Technology,  
Hanoi University of Mining and Geology, Hanoi, Vietnam  
Ngothiphuongthao@humg.edu.vn

<sup>5</sup> Center for the Development of Science and Technology,  
Hanoi University of Mining and Geology, Hanoi, Vietnam  
BuiTienDung204@gmail.com

**Abstract.** Recent technological innovations have led to the available of light-weight Unmanned Aerial Vehicle (UAV) and Structure-from-Motion (SfM) photogrammetry that are successfully applied for 3D topographic surveys. However, application of UAV and SfM for complex topographic areas i.e. open-pit mine areas is still poorly understood. This paper aims to investigate and verify potential application of these techniques for generating Digital Surface Model (DSM) at open-pit coal mine area and assessing its accuracy. For this purpose, the Nui Beo open-pit coal mine located in northeast Vietnam is selected as a case study. Accordingly, a total of 206 photos were captured using DJI Phantom 3 Professional. In addition, 19 ground control points (GCPs) were established using Leica TS09 total station. The accuracy of DSM was assessed using root-mean-square error (RMSE) in X, Y, Z, XY, and XYZ components. The result showed that the DSM model has high accuracy, RMSE on the 12 calibrated GCPs for X, Y, Z, XY, XYZ is 1.1 cm, 1.9 cm, 0.8 cm, 2.2 cm, and 2.3 cm, respectively, whereas RMSE on the 7 checked GCPs is 1.8 cm, 2.4 cm, 3.2 cm, 3.0 cm, and 4.4 cm for X, Y, Z, XY, XYZ components, respectively. We concluded that small UAV and SfM are feasible and valid tools for 3D topographic mapping in complex terrains such as open-pit coal mine areas.

**Keywords:** UAV · Structure-from-Motion · Photogrammetry · Open-pit mine · Nui Beo · Quang Ninh · Vietnam

## 1 Introduction

Direct surveying techniques i.e. Electronic Distance Measurement (EDM) surveys or Total Station (TS) and RTK Global Navigation Satellite System (GNSS) are the most widely used in surveying engineering and volumetric computation at open pit mining due to ability to obtain observations with millimeter accuracy [1]. However, they are cost and time consuming techniques, and in some complex environments, these techniques may be unsafe to workers [2]. Recent technological innovations have provided new alternative techniques for topographic surveying such as Terrestrial Laser Scanning (TLS) and airborne Light Detection and Ranging (LiDAR) or airborne laser scanning (ALS).

For TLS, although this technique is quite straightforward to use and millimeter accuracy could be obtained for objects at short distances, the cost and survey time still are a critical issue because this technique requires many scanning stations. Therefore, TLS may not be suited in projects dealing with complex topographies such as open-pit mines [3]. Regarding LiDAR, the accuracy is heavily influenced by GNSS and Inertial Measurement Unit (IMU) systems. Although accuracy is reported 0.1–0.5 m for vertical and 0.1–0.5 m for horizontal, however, higher vertical errors could occur in areas with complex environments [4].

Recent advancements in robots and GNSS technologies have provided various Unmanned Aerial Vehicles (UAVs) that can be used for topographic surveying. Especially, small and low-cost UAVs with nonmetric digital cameras are becoming a valid and effective alternative surveying technique for topographic reconnaissance and volumetric computation. In addition, the fusion of computer vision and photogrammetry have provided various Structure-from-Motion (SfM) and Multi-View Stereo (MVS) algorithms that have been successfully used for automatic processing UAV images with high quality results [5].

Overall, the main advantage of lightweight UAVs is that they can fly at low altitude with slow speed providing captured photos with fine spatial resolution and users defined temporal resolutions. The SfM algorithms are capable to automatically process orientation and geometry of images as well as camera positions [6]. More specifically, these algorithms have included MVS techniques that enable us to generate various 3D productions from UAV overlapped images, i.e. 3D point cloud and Digital Surface Model (DSM). Consequently, UAV and SfM photogrammetry have successfully been used in various fields i.e. surveying earthwork projects [2], stockpile volumetric [7], topography reconstructions [8], gravel-pit surveying and change estimation [9], ice-cored moraine degradation [10], erosion monitoring [11], precision farming applications [12], and geological mapping [13]. Common conclusions from these works demonstrate that UAV and SfM are new and efficient tools. Nevertheless, accuracy of the topographic mapping and its generated DSM derived from small UAVs and SfM photogrammetry at open pit mines has been rarely assessed and is still poorly understood.

In this work, we extend the body of knowledge by assessing the utility of UAV and SfM photogrammetry for topographic mapping and DSM at complex terrain of open-pit coal mine, with a case study at the Nui Beo coal mine in Quang Ninh province (Vietnam). Accordingly, a DJI Phantom 3 Professional was used to capture images, whereas ground control points were measured by using a Leica TS09 total station. The image processing was carried out using Agisoft®PhotoScan Professional 1.0 (APP). Finally, accuracy assessment was performed and conclusions are given.

## 2 Materials and Methods

### 2.1 Study Site

The study area (Fig. 1) is the Nui Beo open-pit coal mine ( $107^{\circ}7'46''$ ,  $20^{\circ}57'46''$ ), one of the five largest open-cast mines in Vietnam (Nui Beo, Deo Nai, Ha Tu, Cao Son, and Coc Sau), located in the Ha Long city, Quang Ninh province (Vietnam), around 160 km east of the Hanoi city. This mine is operated by the Nui Beo coal joint stock company that belongs to Vietnam National Coal and Mineral Industries (VINACOMIN) group.

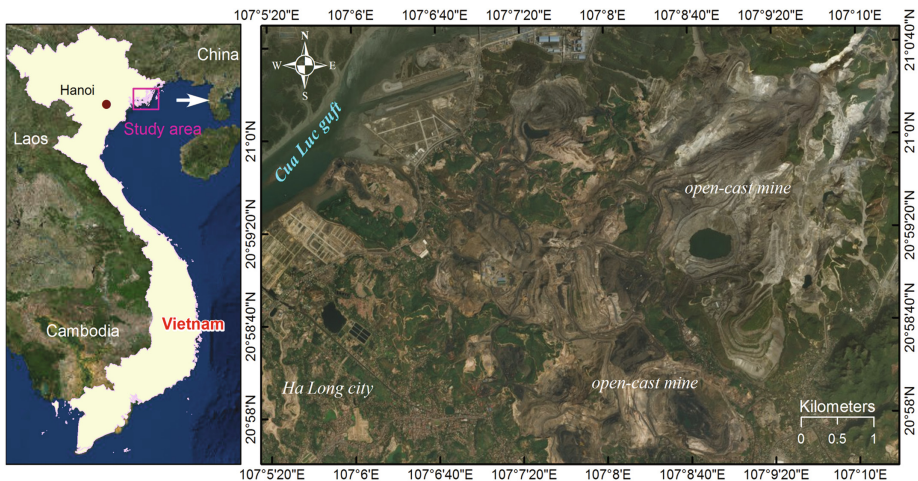


**Fig. 1.** Location of the Nui Beo coal mine.

It is noted that the Quang Ninh province produces 100% exported coals and nearly 90% domestic coals in Vietnam. The Nui Beo open-pit coal mine was designed in 1983 by the Giproruda Institute (former Soviet Union) and has officially operated since May 19, 1989. Total coal production is estimated around 32 million tons [14]. Total mineral coal area is around  $3.75 \text{ km}^2$  for the open-pit coal mines and  $5.6 \text{ km}^2$  for the underground coal mine.

Topographically, the Nui Beo coal mine presents complicated terrain conditions where the center is the opencast mining area, whereas the opening landfill is in the